

# Thirring model at finite density in $2 + 1$ dimensions with stochastic quantization

Jan M. Pawłowski<sup>1,2</sup> and Christian Zielinski<sup>1,\*</sup>

<sup>1</sup>*Institut für Theoretische Physik, Universität Heidelberg, Philosophenweg 16, 69120 Heidelberg, Germany*

<sup>2</sup>*ExtreMe Matter Institute EMMI, GSI, Planckstraße 1, D-64291 Darmstadt, Germany*

(Dated: May 23, 2013)

We consider a generalization of the Thirring model in  $2+1$  dimensions at finite density. We employ stochastic quantization and check for the applicability in the finite density case to circumvent the sign problem. To this end we derive analytical results in the heavy dense limit and compare with numerical ones obtained from a complex Langevin evolution. Furthermore we make use of indirect indicators to check for incorrect convergence of the underlying complex Langevin evolution. The method allows the numerical evaluation of observables at arbitrary values of the chemical potential. We evaluate the results and compare to the  $(0+1)$ -dimensional case.

PACS numbers: 05.50.+q, 71.10.Fd

Keywords: Thirring model, finite density field theory, complex Langevin evolution, stochastic quantization

## I. INTRODUCTION

The sign problem remains one of the biggest challenges of lattice field theory until this day. It is caused by a highly oscillatory and complex path integral measure after introducing a chemical potential  $\mu$ . This renders many theories, like four-dimensional quantum chromodynamics (QCD), inaccessible by common simulation algorithms in wide regions of the phase diagram. Many solutions have been proposed, see e.g., [1–8]. However, reliable numerical calculations in theories with a severe sign problem remain extremely challenging.

One of the approaches to the sign problem is stochastic quantization [9], i.e., a complex Langevin evolution [10]. For a review of stochastic quantization see e.g., [11], and for its application to the finite density case refer to [3]. It has been applied to many theories suffering from a severe sign problem, often successfully [12–18]. It was also applied outside the context of finite density calculations, e.g., quantum fields in nonequilibrium [19] and in real time [20, 21]. However, there are cases known where the complex Langevin evolution converges towards unphysical fixed points [22, 23]. Starting from early studies of complex Langevin evolutions [24–26] until this day, the convergence properties of Langevin equations generalized to the complex case are not well understood. In this work we focus on the stochastic quantization of the Thirring model at finite density in  $2 + 1$  dimensions, cf. [27]. This serves as a toy model for the matter sector of QCD. Furthermore, the  $(2 + 1)$ -dimensional model appears in effective theories of high temperature superconductors and graphene, see e.g., references given in [28].

Here we extend the  $(0 + 1)$ -dimensional studies carried out in [29]. In  $2 + 1$  dimensions we lose the analytic benchmarks which facilitated the interpretation of the

numerical results with stochastic quantization in  $0 + 1$  dimensions. Still, we can exploit the similarities to the lower-dimensional case. Further benchmarks of our numerical results are given by those in the heavy dense limit, as introduced in [30]. This limit describes the regime of large fermion masses and large chemical potentials. In addition, we evaluate indirect indicators, namely the consistency requirements presented in [31–33] and the analyticity of the fermion condensate at  $\mu^2 = 0$ , cf. [13].

The paper is organized as follows: In Sec. II we introduce a generalized Thirring model in the continuum and on the lattice. We also formulate the associated Langevin equation. In Sec. III we employ the heavy dense limit to derive numerous analytical results. At the end of the section we introduce indirect indicators of correct convergence, namely analyticity of observables at  $\mu^2 = 0$  and a set of consistency conditions. In Sec. IV we discuss numerical results and use the analytical results among other indicators as a benchmark to evaluate the complex Langevin evolution. Finally in Sec. V we discuss and summarize our findings.

## II. THE GENERALIZED THIRRING MODEL

### A. Continuum formulation

We begin with a short recapitulation of the model, which we introduced in [29]. It is a generalization of the historical  $1 + 1$  dimensional Thirring model [34], but formulated in  $d$  dimensions with  $N_f$  fermion flavors at finite density. The Euclidean Lagrangian reads

$$\mathcal{L}_\Psi = \sum_{i=1}^{N_f} \bar{\Psi}_i (\not{\partial} + m_i + \mu_i \gamma_0) \Psi_i + \frac{g^2}{2N_f} \left( \sum_{i=1}^{N_f} \bar{\Psi}_i \gamma_\nu \Psi_i \right)^2. \quad (1)$$

\* Permanent address: Division of Mathematical Sciences, Nanyang Technological University, Singapore 637371

Here  $i = 1, \dots, N_f$  is a flavor index,  $m_i$  and  $\mu_i$  are the bare mass and bare chemical potential of the respective flavor and  $g^2$  is the bare coupling strength. The  $\gamma$  matrices satisfy  $\{\gamma_\mu, \gamma_\nu\} = 2\delta_{\mu\nu}\mathbb{1}$ .

In  $d = 2 + 1$  dimensions,  $\bar{\Psi}$  and  $\Psi$  denote four-component spinors. While it is possible to use an irreducible two-dimensional representation of the Dirac algebra, this representation does not allow for a chiral symmetry in the massless case. See [28] for details and a discussion of symmetries. It is noted that the model also shows breaking of chiral symmetry at vanishing chemical potential [35].

We reformulate the generalized Thirring model using an auxiliary field and integrate out the fermionic degrees of freedom. We find for the partition function

$$Z = \int \mathcal{D}A \left( \prod_i \det K_i \right) e^{-S_A} = \int \mathcal{D}A e^{-S_{\text{eff}}},$$

$$S_A = N_f \beta \int_0^{1/T} dt \int d^{d-1} \mathbf{x} A_\nu^2 \quad (2)$$

with temperature  $T$ , fermionic term  $K_i = \not{\partial} + i\not{A} + m_i + \mu_i \gamma_0$  and  $S_{\text{eff}} = S_A - \sum_i \text{Tr} \log K_i$ . The fermion determinant obeys

$$\det K_i(\mu) = [\det K_i(-\mu^*)]^*, \quad (3)$$

yielding in general a complex action. The sign problem can be avoided by taking the absolute value of the fermion determinant. This corresponds to an isospin chemical potential and is also referred to as the phase-quenched case. We also note that observables shall become independent of the chemical potential  $\mu$  up to some threshold  $\mu_c$  in the zero-temperature limit. This goes under the name of the Silver Blaze problem [36].

## B. Lattice formulation

We consider the generalized Thirring model in  $2 + 1$  dimensions on a space-time lattice with  $N_t$  time slices and  $N_s$  slices in spatial direction. Furthermore, we require that  $N_t$  be even [29]. The spatial volume and the space-time volume are denoted by

$$V = N_s^2, \quad \Omega = N_t N_s^2. \quad (4)$$

We use staggered fermions [37–40], where the number of staggered fermion fields—denoted also as lattice flavors—is given by  $\mathcal{N}$ . The introduction of a chemical potential follows the prescription by Hasenfratz and Karsch [41]. In the following, all dimensionful quantities are measured in appropriate powers of  $a$ , so that we only deal with dimensionless parameters.

In three dimensions,  $\mathcal{N}$  staggered fermion flavors correspond to  $N_f = 2\mathcal{N}$  continuum flavors [27] as each staggered fermion field encodes two tastes. In principle the

partition function for a single continuum flavor can be obtained by taking the square root of the fermion determinant, but it is still under debate if this rooting prescription is consistent [42].

In  $d = 2 + 1$  dimensions (where generalizations to arbitrary  $d$  are evident), the lattice action we employ reads

$$S = \sum_{x,y,i} \bar{\chi}_i(x) K_i(x,y) \chi_i(y) + \frac{\mathcal{N}\beta}{2} \sum_{x,\nu} A_\nu^2(x). \quad (5)$$

Here  $\bar{\chi}_i$  and  $\chi_i$  denote staggered fermion fields with flavor index  $i = 1, \dots, \mathcal{N}$ , and the sums extend over  $x, y = 1, \dots, \Omega$  and  $\nu = 0, \dots, d-1$ . The fermion matrix reads

$$K_i(x,y) = \frac{1}{2} \sum_{\nu=0}^{d-1} \varepsilon_\nu(x) [(1 + iA_\nu(x)) e^{\mu_i \delta_{\nu 0}} \delta_{x+\hat{\nu},y} - (1 - iA_\nu(y)) e^{-\mu_i \delta_{\nu 0}} \delta_{x-\hat{\nu},y}] + m_i \delta_{xy} \quad (6)$$

with staggered phase factor

$$\varepsilon_\nu(x) = (-1)^{\sum_{i=0}^{\nu-1} x_i} \quad (7)$$

and  $\hat{\nu}$  denoting a unit vector in  $\nu$  direction, cf. [27, 43]. We impose periodic boundary conditions in spatial and antiperiodic boundary conditions in temporal direction. The lattice partition function is, like in the continuum in (2), given by

$$Z = \prod_{x,v} \int dA_v(x) \left( \prod_i \det K_i \right) e^{-S_A}, \quad (8)$$

where  $S_A = \frac{1}{2} \mathcal{N} \beta \sum_{x,\nu} A_\nu^2(x)$ . The central observables in our analysis are the fermion density, the fermion condensate, the energy density and the phase factor of the fermion determinant. In the following, sums over flavor indices are not implied. The fermion density of flavor  $i$  is given by

$$\langle n_i \rangle = \frac{1}{\Omega} \left( \frac{\partial \log Z}{\partial \mu_i} \right)_{V,T} = \frac{1}{\Omega} \left\langle \text{Tr} \left( \frac{\partial K_i}{\partial \mu_i} K_i^{-1} \right) \right\rangle. \quad (9)$$

The fermion condensate follows from

$$\langle \bar{\chi}_i \chi_i \rangle = \frac{1}{\Omega} \left( \frac{\partial \log Z}{\partial m_i} \right)_{V,T,\mu_i} = \frac{1}{\Omega} \langle \text{Tr} K_i^{-1} \rangle, \quad (10)$$

and the energy density reads

$$\langle \varepsilon_i \rangle = - \left( \frac{\partial \log Z}{\partial N_t} \right)_{V,\mu_i} + \mu_i \langle n_i \rangle. \quad (11)$$

Usually we normalize the latter one to  $\langle \varepsilon_i \rangle (\mu = 0) = 0$ .

The phase factor of the fermion determinant is defined by  $\exp(i\phi) = \det K / |\det K|$  with phase  $\phi$ . For  $\mathcal{N}$  degenerated staggered fermion flavors we set  $K_i = K$ . The expectation value of  $\exp(i\mathcal{N}\phi)$  [44, 45] follows in the  $\mathcal{N}$  flavor phase-quenched theory from

$$\langle e^{i\mathcal{N}\phi} \rangle_{\mathcal{N}}^{\text{pq}} = \frac{Z_{\mathcal{N}}}{Z_{\mathcal{N}}^{\text{pq}}} \in [0, 1], \quad (12)$$

where  $Z_{\mathcal{N}}$  is given by (8) and  $Z_{\mathcal{N}}^{\text{pq}}$  denotes the phase-quenched partition function. The expectation value of the fermion phase factor is a measure of the sign problem, where smaller values indicate a more severe problem.

### C. Complex Langevin equation

To deal with the associated sign problem we apply stochastic quantization [9], namely a complex Langevin evolution [10], to the Thirring model at finite density. To this end we determine the stationary solution of the corresponding Langevin equation, which reads

$$\frac{\partial}{\partial \Theta} A_{\nu}(x, \Theta) = -\frac{\delta S_{\text{eff}}[A]}{\delta A_{\nu}(x, \Theta)} + \sqrt{2} \eta_{\nu}(x, \Theta). \quad (13)$$

Here  $\Theta$  denotes fictitious time, and  $\eta_{\nu}(x, \Theta)$  is a Gaussian noise with

$$\begin{aligned} \langle \eta_{\nu}(x, \Theta) \rangle &= 0, \\ \langle \eta_{\nu}(x, \Theta) \eta_{\sigma}(x', \Theta') \rangle &= \delta_{\nu\sigma} \delta(x - x') \delta(\Theta - \Theta'). \end{aligned} \quad (14)$$

We use an adaptive first-order stepsize integration scheme [27, 46, 47], where the stepsize  $\epsilon_L$  is adjusted with respect to the modulus of the drift term.

For the numerical treatment of the Langevin equation we use a first-order integration scheme. Our discretization of (13) reads

$$\begin{aligned} A_{\nu}(x, \Theta + \epsilon_L) &= \\ A_{\nu}(x, \Theta) + \epsilon_L D_{\nu}(x, \Theta) + \sqrt{2\epsilon_L} \eta_{\nu}(x, \Theta), \end{aligned} \quad (15)$$

where  $D_{\nu}(x, \Theta) = -\text{d}S_{\text{eff}}/\text{d}A_{\nu}(x, \Theta)$  is the drift term and  $\epsilon_L$  the (adaptive) integration stepsize. The drift term takes the explicit form

$$\begin{aligned} D_{\nu}(x, \Theta) &= -\mathcal{N}\beta A_{\nu}(x, \Theta) \\ &+ \frac{i}{2} \varepsilon_{\nu}(x) \sum_i K_i^{-1}(x + \hat{\nu}, x) e^{\mu_i \delta_{v0}} \\ &+ \frac{i}{2} \varepsilon_{\nu}(x + \hat{\nu}) \sum_i K_i^{-1}(x, x + \hat{\nu}) e^{-\mu_i \delta_{v0}}, \end{aligned} \quad (16)$$

cf. [27]. The stepsize is updated after each integration step according to

$$\epsilon_L \equiv \epsilon_L(\Theta) = \frac{\delta}{\max_{x,\nu} |D_{\nu}(x, \Theta)|}. \quad (17)$$

Typically we use  $\delta = 10^{-2}$ , see also [29].

For a correctly converging complex Langevin evolution we can generalize the real noise to an imaginary noise in (13) while keeping expectation values unchanged [27]. We parametrize the complex noise using the replacement

$$\eta_{\nu}(x, \Theta) \rightarrow \sqrt{\mathcal{I} + 1} \text{Re} \eta_{\nu}(x, \Theta) + i\sqrt{\mathcal{I}} \text{Im} \eta_{\nu}(x, \Theta) \quad (18)$$

with  $\mathcal{I} \geq 0$ . Furthermore, we require that

$$\begin{aligned} \langle \text{Re} \eta_{\nu}(x, \Theta) \text{Re} \eta_{\sigma}(x', \Theta') \rangle &= \langle \text{Im} \eta_{\nu}(x, \Theta) \text{Im} \eta_{\sigma}(x', \Theta') \rangle \\ &= \delta_{\nu\sigma} \delta(x - x') \delta(\Theta - \Theta') \end{aligned} \quad (19)$$

and

$$\langle \text{Re} \eta_{\nu}(x, \Theta) \text{Im} \eta_{\sigma}(x', \Theta') \rangle = 0. \quad (20)$$

While maintaining numerical stability, we check if observables turn out to be independent of  $\mathcal{I}$ .

## III. ANALYTICAL RESULTS

In the following we derive approximate expressions for some observables in the lattice Thirring model in  $d$  dimensions. We begin with a hopping parameter expansion and then take the so-called heavy dense limit in Sec. III B. This renders the model effectively one-dimensional and allows us to obtain a simple expression for the fermion determinant. Later we discuss an extended version in Sec. III F.

### A. Hopping parameter expansion

Applying a hopping parameter expansion to the fermion determinant in (8) yields

$$\frac{\det K}{m^{\Omega}} = \prod_{\ell} \prod_{\{C_{\ell}\}} (1 - \kappa^{\ell} \gamma_{C_{\ell}} \mathbf{P}_{C_{\ell}}). \quad (21)$$

Here  $\kappa = 1/(2m)$  is the hopping parameter,  $\{C_{\ell}\}$  are closed contours of perimeter  $\ell$ ,  $n$  is the number of times a given contour is traced out and  $\mathbf{P}_{C_{\ell}}$  is the product of hopping terms  $M(x, y)$  at  $\mu = 0$  along the given contour  $C_{\ell}$ . The matrix elements  $M(x, y)$  read

$$\begin{aligned} M(x, y) &= -\sum_{\nu=0}^{d-1} \varepsilon_{\nu}(x) [(1 + iA_{\nu}(x)) \delta_{x+\hat{\nu}, y} \\ &\quad - (1 - iA_{\nu}(y)) \delta_{x-\hat{\nu}, y}], \end{aligned} \quad (22)$$

compare with the fermion matrix in (6). Furthermore, we represent the dependence on the chemical potential explicitly via

$$\gamma_{C_{\ell}} = [-\exp(\mu N_t)]^{\odot C_{\ell}}, \quad (23)$$

where

$$\odot C_{\ell} \in \mathbb{Z} \quad (24)$$

denotes the temporal winding number of the path  $C_{\ell}$  counted in positive direction. The minus sign in (23) stems from antiperiodic temporal boundary conditions.

### B. Heavy dense limit

The heavy dense limit projects out the leading contributions of the hopping parameter expansion in the limit of a large mass  $m$  and large chemical potential  $\mu$ . This limit was introduced in [30] and employed e.g., in [15, 48–53]. It is defined by

$$\kappa \rightarrow 0, \quad \mu \rightarrow \infty, \quad \kappa e^\mu \text{ fixed.} \quad (25)$$

In this regime the fermion determinant is dominated by contributions from Polyakov loops in positive time direction with  $\mathcal{C} = 1$ , see (24). Due to the absence of spatial paths, the model is effectively one dimensional. The fermionic contribution  $\det \mathcal{K}$  in this limit reads

$$\frac{\det \mathcal{K}}{m^\Omega} = \prod_{C \in \mathbb{P}} (1 + \xi \mathbf{P}_C), \quad (26)$$

where  $\mathbb{P}$  denotes the set of Polyakov loops and

$$\xi \equiv \zeta^{N_t}, \quad \zeta \equiv \kappa e^\mu. \quad (27)$$

Let  $\mathcal{P}_{\mathbf{x}}$  denote a Polyakov loop

$$\mathcal{P}_{\mathbf{x}} = \prod_{t=1}^{N_t} (1 + iA_0(t, \mathbf{x})) \quad (28)$$

starting and ending in the space point  $\mathbf{x}$ . We can then express the fermion determinant in the regime of  $m$  and  $\mu$  being large by

$$\det \mathcal{K} = m^\Omega \prod_{\mathbf{x}} (1 + \xi \mathcal{P}_{\mathbf{x}}), \quad (29)$$

where  $\Omega$  is the space-time volume defined in (4). Note that in this limit the relation in (3) is violated. Due to this approximation we will find  $\langle n \rangle_{\mu=0} \rightarrow 0$  only for  $m \rightarrow \infty$ . In Sec. III F we introduce a modified version of this limit, which preserves this relation.

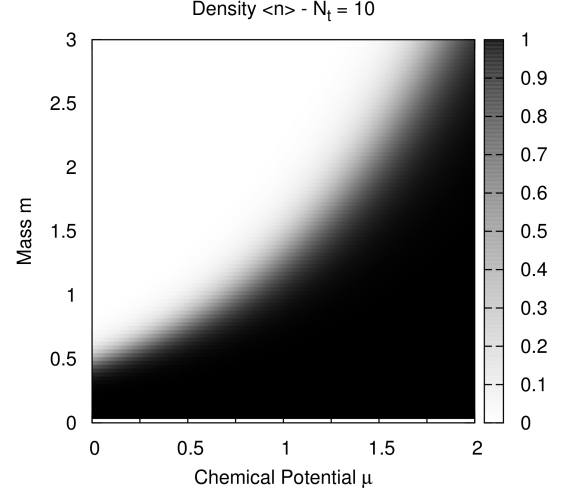
### C. The case of one flavor

By replacing the full fermion determinants in (8) with the simpler expression in (29), we can derive analytical expressions for several observables of interest. We begin with one flavor and later generalize to more flavors. In the heavy dense limit the partition function can be integrated exactly, and we find

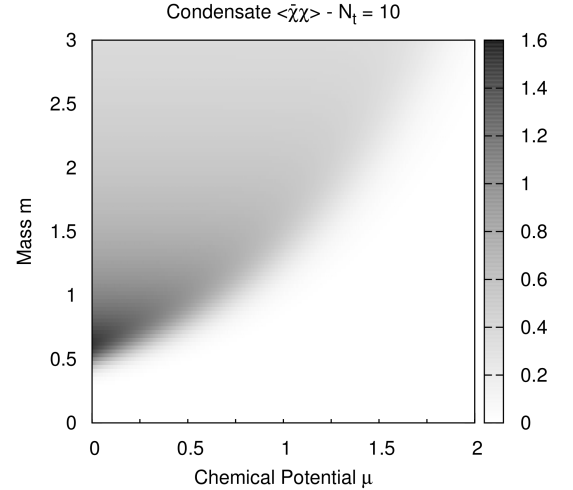
$$\mathcal{Z}_1 = \int_{-\infty}^{\infty} \prod_{x,v} dA_v(x) \det \mathcal{K} e^{-S_A} = \frac{(1 + \xi)^V}{(2\kappa)^\Omega} \left( \frac{2\pi}{\beta} \right)^{\frac{\Omega d}{2}}. \quad (30)$$

Using (9) and (10) the fermion density and condensate read

$$\langle n \rangle = \frac{1}{1 + \frac{1}{\xi}}, \quad \langle \bar{\chi} \chi \rangle = \frac{2\kappa}{1 + \xi}. \quad (31)$$



(a) Plot of the fermion density  $\langle n \rangle$ .



(b) Plot of the fermion condensate  $\langle \bar{\chi} \chi \rangle$ .

Figure 1: The phase structure in the heavy dense limit for one flavor.

We point out that the exact  $(0+1)$ -dimensional results derived in [29] reproduce the above results in the corresponding limit. Applying (11), the normalized energy density reads

$$\langle \varepsilon \rangle = \frac{(\xi - \kappa^{1/T}) \log \kappa^{-1}}{(1 + \kappa^{1/T})(1 + \xi)}, \quad (32)$$

where we identify the temperature with  $T = N_t^{-1}$ . Furthermore, we find

$$c_V = \frac{1}{VT^2} \left( \frac{\partial^2 \log \mathcal{Z}_1}{\partial N_t^2} \right)_{V, \mu} = \frac{\xi \log^2 \zeta}{T^2 (1 + \xi)^2} > 0 \quad (33)$$

for the heat capacity. The corresponding mechanical equation of state  $PV = T \log \mathcal{Z}_1$  takes the form

$$P = \log \left[ \frac{(1 + \xi)^{1/T}}{2\kappa} \left( \frac{2\pi}{\beta} \right)^{d/2} \right] \quad (34)$$

with  $P$  denoting pressure.

Figure 1 shows the phase structure in the heavy dense limit. Note that  $\beta$  dropped out in most considered observables. For large  $N_t$  we find two well-separated phases, where the system is in a condensed phase for large  $\mu$ .

In the limit of vanishing temperature we find

$$\begin{aligned} \langle n \rangle_{T=0} &= \Theta(\mu - \mu_c), \\ \langle \bar{\chi} \chi \rangle_{T=0} &= 2\kappa \Theta(\mu_c - \mu), \\ \langle \varepsilon \rangle_{T=0} &= \mu_c \Theta(\mu - \mu_c), \end{aligned} \quad (35)$$

where  $\Theta$  is the Heaviside step function and the critical chemical potential onset is found to be  $\mu_c = \log(2m)$ . Note that  $\mu_c > 0$  in the heavy dense regime. The model clearly exhibits Silver Blaze behavior as mentioned in Sec. I.

#### D. The case of two flavors

We continue with determining the partition function for two flavors in the heavy dense limit. For nondegenerated flavors we label the parameters  $\kappa$ ,  $\mu$  and  $\xi$  with a flavor index  $i \in \{1, 2\}$  and find after an exact integration

$$\begin{aligned} \mathcal{Z}_2 &= \int_{-\infty}^{\infty} \prod_{x,v} dA_v(x) \det \mathcal{K}_1 \det \mathcal{K}_2 e^{-S_A} \\ &= \frac{(1 + \xi_1 + \xi_2 + \xi_1 \xi_2 \Delta)^V}{(4\kappa_1 \kappa_2)^\Omega} \left( \frac{\pi}{\beta} \right)^{\frac{\Omega d}{2}}, \end{aligned} \quad (36)$$

where we introduce

$$\Delta = \left( 1 - \frac{1}{2\beta} \right)^{N_t} \quad (37)$$

for brevity. For simplicity we quote the observables only in the case of degenerated flavors and a common chemical potential, i.e.,  $\kappa_i = \kappa$ ,  $\mu_i = \mu$  and  $\xi_i = \xi$ . The generalization to nondegenerated flavors is straightforward. The total fermion density is given by

$$\langle n \rangle = \frac{2\xi(1 + \xi\Delta)}{1 + 2\xi + \xi^2\Delta} \quad (38)$$

with  $\langle n \rangle \rightarrow 2$  for  $\mu \rightarrow \infty$  (if  $\beta \neq 1/2$ ), while the fermion condensate reads

$$\langle \bar{\chi} \chi \rangle = \frac{4\kappa(1 + \xi)}{1 + 2\xi + \xi^2\Delta}. \quad (39)$$

The mechanical equation of state takes the form

$$P = \log \left[ \frac{(1 + 2\xi + \xi^2\Delta)^{1/T}}{4\kappa^2} \left( \frac{\pi}{\beta} \right)^{d/2} \right]. \quad (40)$$

Like in  $0 + 1$  dimensions [29] we find a plateau in the density, condensate and energy density for  $\mathcal{N} = 2$ . They become visible for couplings of the order  $\beta \approx 1/2$ , see Fig. 7. For the special case of  $\beta = 1/2$  (i.e.  $\Delta = 0$ ), the density never goes into full saturation for  $\mu \rightarrow \infty$ , but is stuck on the plateau. These structures can be understood in the  $(0 + 1)$ -dimensional continuum case [29], see also [54].

*Phase-quenched case.* We also consider the partition function with a phase-quenched fermion determinant as mentioned in Sec. II B. Then in the case of two degenerated flavors, the partition function reads

$$\begin{aligned} \mathcal{Z}_2^{\text{pq}} &= \int_{-\infty}^{\infty} \prod_{x,v} dA_v(x) |\det \mathcal{K}|^2 e^{-S_A} \\ &= \frac{1}{(2\kappa)^{2\Omega}} \left[ (1 + 2\xi + \xi^2\Delta_{\text{pq}}) \left( \frac{\pi}{\beta} \right)^{N_t d/2} \right]^V \end{aligned} \quad (41)$$

with

$$\Delta_{\text{pq}} = \left( 1 + \frac{1}{2\beta} \right)^{N_t}. \quad (42)$$

The observables are of the same form as in the full theory with  $\Delta$  replaced by  $\Delta_{\text{pq}}$ .

*Phase factor.* The previous results allow us to derive an analytical expression for the expectation value of the phase factor of the fermion determinant in the two-flavor theory. It serves as a measure for the severity of the sign problem. We find

$$\langle e^{2i\phi} \rangle_{\mathcal{N}=2}^{\text{pq}} = \frac{\mathcal{Z}_2}{\mathcal{Z}_2^{\text{pq}}} = e^{-V/V_0}, \quad (43)$$

where we define

$$V_0 = \log \left( \frac{1 + 2\xi + \xi^2\Delta_{\text{pq}}}{1 + 2\xi + \xi^2\Delta} \right). \quad (44)$$

As expected, the sign problem gets more severe for larger lattices. In the limit of large chemical potentials the expectation value approaches

$$\lim_{\mu \rightarrow \infty} \langle e^{2i\phi} \rangle_{\mathcal{N}=2}^{\text{pq}} = \left( \frac{2\beta - 1}{2\beta + 1} \right)^\Omega. \quad (45)$$

We see that the choice of  $\beta$  has a significant impact on the severity of the sign problem. In the heavy dense limit we find that it is most severe for  $\beta = 1/2$ .

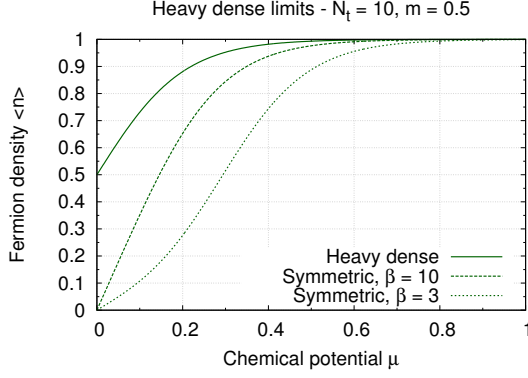


Figure 2: The density in the strict and in the symmetric heavy dense limit.

### E. The case of $\mathcal{N}$ flavors

Finally, we generalize (30) to an arbitrary number of  $\mathcal{N}$  degenerated flavors by raising the fermion determinant to the power of  $\mathcal{N}$  in the partition function. We obtain

$$\mathcal{Z}_{\mathcal{N}} = \frac{1}{(2\kappa)^{\mathcal{N}\Omega}} \left( \frac{2\pi}{\mathcal{N}\beta} \right)^{\frac{\Omega d}{2}} \times \left[ \sum_{k=0}^{\mathcal{N}} \binom{\mathcal{N}}{k} \Lambda_k \xi^k U^{N_t} \left( \frac{1-k}{2}, \frac{3}{2}, \frac{\mathcal{N}\beta}{2} \right) \right]^V \quad (46)$$

in the heavy dense limit, where we introduce

$$\Lambda_k = \left( \frac{2}{\mathcal{N}\beta} \right)^{\frac{N_t(k-1)}{2}}. \quad (47)$$

Here  $\Gamma(z)$  denotes Euler's gamma function, and  $U(a, b, z)$  is the confluent hypergeometric function of the second kind [55], also known as Kummer's function. We do not want to quote the observables here explicitly, but as required they reproduce previous results for  $\mathcal{N} = 1, 2$ . From the expressions for the density and condensate we obtain the relation

$$\frac{\langle \bar{\chi} \chi \rangle}{\mathcal{N}} = 2\kappa \left( 1 - \frac{\langle n \rangle}{\mathcal{N}} \right). \quad (48)$$

In this general case we find up to  $\mathcal{N} - 1$  intermediate plateaus in the observables.

### F. Symmetric heavy dense limit

The heavy dense limit given by (25) violates the relation in (3). In the following, we consider a model which restores the determinant symmetry but is not a strict limit of the generalized Thirring model. Besides

the Polyakov loops in positive time direction with their characteristic  $\exp(\mu)$  dependence, we will also consider the ones in negative Polyakov direction with an  $\exp(-\mu)$  dependence. In this sense we speak of a symmetrized version of the heavy dense limit.

In this model the fermion determinant  $\det \mathfrak{K}$  has the form

$$\det \mathfrak{K} = \prod_{\mathbf{x}} \left( 1 + \xi_f \prod_{t=1}^{N_t} (1 + iA_0(\mathbf{x}, t)) \right) \times \prod_{\mathbf{x}} \left( 1 + \xi_b \prod_{t=1}^{N_t} (1 - iA_0(\mathbf{x}, t)) \right), \quad (49)$$

where we introduce  $\xi_f \equiv (\kappa e^\mu)^{N_t}$  and  $\xi_b \equiv (\kappa e^{-\mu})^{N_t}$ , compare with (29). The respective partition function reads

$$\mathcal{Z}_1^{\text{sym}} = \int_{-\infty}^{\infty} \prod_{x,v} dA_v(x) \det \mathfrak{K} e^{-S_A} = \frac{1}{(2\kappa)^\Omega} \left( \frac{2\pi}{\beta} \right)^{\frac{\Omega d}{2}} (1 + \xi_f + \xi_b + \Delta_{\text{sym}})^V \quad (50)$$

with shorthand notation

$$\Delta_{\text{sym}} = \kappa^{2N_t} \left( 1 + \frac{1}{\beta} \right)^{N_t}. \quad (51)$$

For small  $\mu$  the observables now receive additional contributions. The density reads

$$\langle n \rangle = \frac{\xi_b - \xi_f}{1 + \xi_f + \xi_b + \Delta_{\text{sym}}} \quad (52)$$

and vanishes exactly at  $\mu = 0$ . The fermion condensate is given by

$$\langle \bar{\chi} \chi \rangle = \frac{2\kappa (1 - \Delta_{\text{sym}})}{1 + \xi_f + \xi_b + \Delta_{\text{sym}}} \quad (53)$$

and the equation of state takes the form

$$P = \log \left[ \frac{(1 + \xi_f + \xi_b + \Delta_{\text{sym}})^{1/T}}{2\kappa} \left( \frac{2\pi}{\beta} \right)^{d/2} \right]. \quad (54)$$

The quantitative differences between the ordinary and the symmetric heavy dense limits are small in the regime of large fermion masses and large chemical potentials due to the exponential suppression of the additional contributions. For small  $m$  they alter the behavior of observables massively, see Fig. 2. However, for very small  $m$  the results again remain unphysical. Spatial contributions to the fermion determinant become important, thus rendering the model invalid.



## G. Analyticity in $\mu^2$

For observables which are even in  $\mu$  we can consider the analytic continuation to  $\mu^2 < 0$ , corresponding to an imaginary chemical potential. An example for such an observable is the fermion condensate  $\langle \bar{\chi}\chi \rangle$ . Due to the relation in (3) the theory is free of a sign problem in this case and we can make use of a real Langevin evolution. For  $\mu^2 > 0$  we employ a complex Langevin evolution.

Assuming that the complex Langevin evolution is correct,  $\langle \bar{\chi}\chi \rangle$  should be analytic in  $\mu^2$ . Then any nonanalytical behavior at  $\mu^2 = 0$  has to be caused by incorrect convergence. We will check this criterion in Sec. IV F, compare also with [13].

## H. Consistency conditions

In [31–33] the authors derived an infinite tower of identities able to indicate the correctness of complex Langevin evolutions. They could show that for all entire holomorphic observables  $\mathcal{O}$  the relation  $\langle L_\nu(x) \mathcal{O} \rangle = 0$  holds if and only if the evolution is converging correctly. Here

$$L_\nu(x) = \left( \frac{d}{dA_\nu(x)} + D_\nu(x) \right) \frac{d}{dA_\nu(x)} \quad (55)$$

is the Langevin operator (summation over  $\nu$  is not implied in this subsection). A simple finite set of observables is defined by  $\mathcal{O}_\nu(x, k) = \exp(ikA_\nu(x))$  with  $k \in \mathbb{Z}$ , yielding a necessary condition for correctness. In Sec. IV F we will check if

$$\langle L_\nu \mathcal{O}_\nu \rangle = \left\langle ik [ik + D_\nu(x)] e^{ikA_\nu(x)} \right\rangle = 0 \quad (56)$$

holds for a wide range of parameters.

# IV. NUMERICAL RESULTS

## A. Implementation

We solve the Langevin equation numerically using the adaptive stepsize algorithm described in Sec. II C. The implementation uses the GNU Scientific Library [56]. The code allows the calculation of the density, the condensate, the phase factor of the fermion determinant, and the consistency conditions of Sec. IV F for the full generalized Thirring model. Furthermore, there is the option to carry out calculations at purely imaginary chemical potential and in the phase-quenched case.

To numerically determine observables we begin with a hot start, i.e., we randomly initialize the auxiliary field. This is followed by 5000 thermalization steps. To evaluate the observables we sample the field configuration typically  $\mathcal{O}(10^4)$  times. Like in the  $(0+1)$ -dimensional case [29], we estimate the error with a bootstrap analysis

[57], as the resulting error bounds generally prove to be more reliable. However, in some cases we observe that the actual error is underestimated.

## B. Comparison to phase-quenched case

In Fig. 3 we find a typical example for numerical results of the density and the condensate in the full as well as the phase-quenched case. The error bars are included, but are often too small to be spotted with the naked eye. Although we only have  $N_t = 8$  time slices, we can already find hints for Silver Blaze behavior. The onset to the condensed phase for the full theory generally lies higher than in the phase-quenched case.

The phase factor of the fermion determinant can serve as a measure for the severity of the sign problem and can be found in Fig. 4. We see that for large  $\beta$  it is less pronounced, but still quickly approaches zero for increasing  $\mu$ .

## C. Evaluation in the heavy dense limit

In the analytical heavy dense limit in Sec. III C, the coupling factorizes, thus rendering the density and the condensate independent of  $\beta$ . However, in Fig. 5 we can see that the numerical results for the full theory show a dependence on  $\beta$  even for extremely large masses. Furthermore, the gap between numerics and the analytical heavy dense limit results seem to persist even when increasing  $m$  by several magnitudes. For smaller  $\beta$  this deviation is more pronounced, while for increasing  $\beta$  we can see how the curves are approaching each other asymptotically, similar to the  $(0+1)$ -dimensional case [29].

It is difficult to separate the different contributions to this gap, as we are comparing an approximate analytical result with an algorithm for the full generalized Thirring model, whose correctness we aim to check. In the  $(0+1)$ -dimensional case we already found a real deviation to theoretical results for small  $\beta$ , and something comparable can potentially also happen in the  $(2+1)$ -dimensional case.

## D. Coupling parameter dependence

In Fig. 6 we plotted the numerically evaluated observables as functions of  $\beta$ . For small  $\beta$  it is more difficult to obtain reliable results due to spikes caused by numerical instabilities. For very large  $\beta$  the results from the full theory approach the phase-quenched calculations. As the heavy dense limit makes no prediction about the  $\beta$  dependence, the interpretation of the findings is difficult.

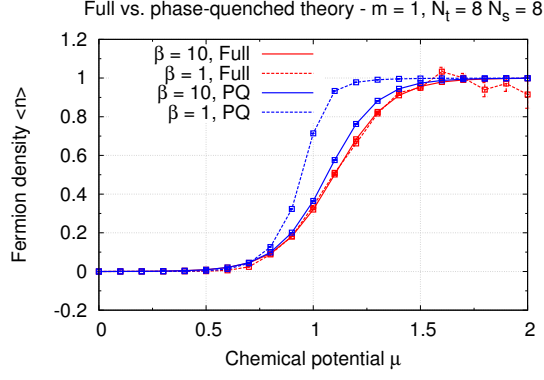
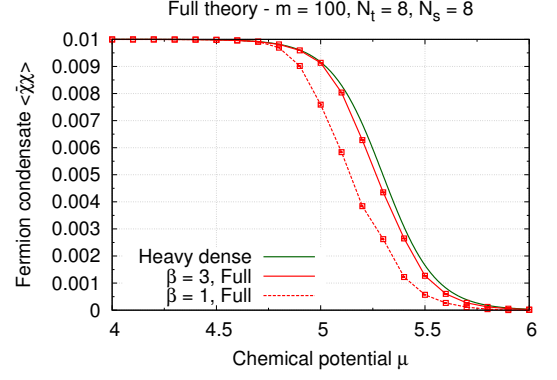
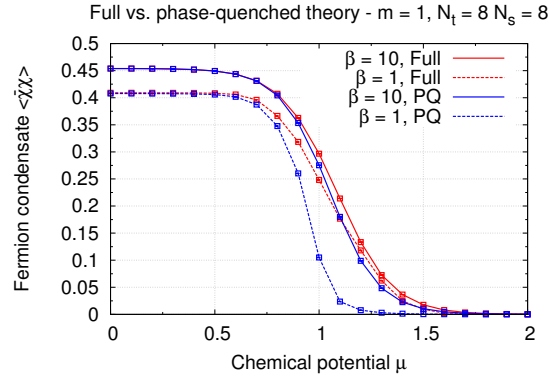
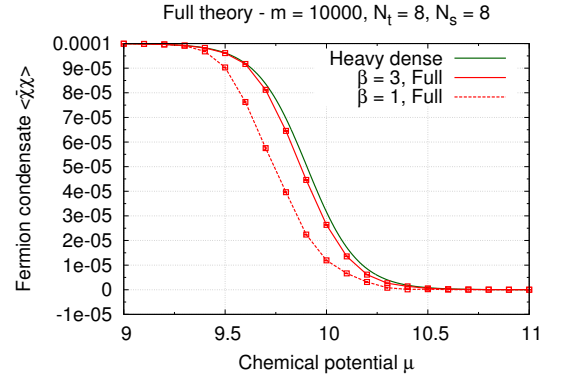
(a) Density  $\langle n \rangle$ .(a) For mass  $m = 10^2$ .(b) Condensate  $\langle \bar{\chi}\chi \rangle$ .(b) For mass  $m = 10^4$ .Figure 3: Full and phase-quenched numerical results for  $\beta = 1, 10$ .

Figure 5: Numerical results and heavy dense limit of the condensate for large masses.

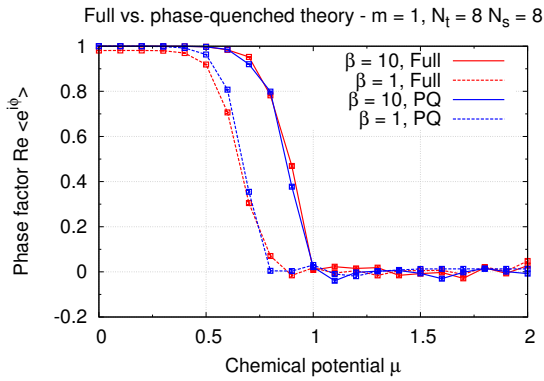


Figure 4: Severity of the sign problem.

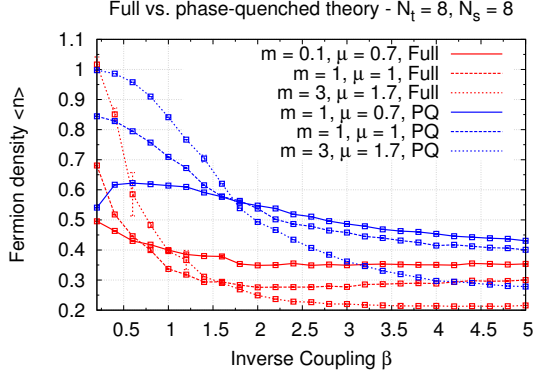
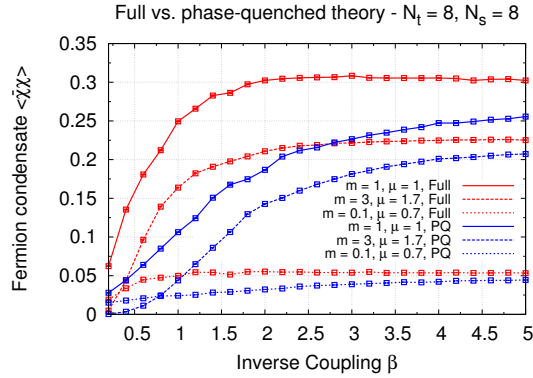
## E. Several flavors

In Fig. 7 we can find the density and the condensate in the case of  $\mathcal{N} = 2$  staggered fermion flavors at a coupling of  $\beta = 0.6$ . As we saw in Secs. IIID and IIIE, in a certain range of  $\beta$  these observables show up to  $\mathcal{N} - 1$  plateaus in the analytical heavy dense results. However, we observe that the numerical results for the full theory do not reproduce these plateau structures at any value of  $\beta$ . Only when considering very large  $\beta$  is the theoretical curve free of these structures, and the complex Langevin evolution approaches the correct result. This finding is in agreement with [29].

## F. Consistency conditions

The numerical check of the consistency conditions of Sec. IIIF for the  $\mathcal{O}_\nu(x, k)$  observable yields several vio-



(a) Fermion density  $\langle n \rangle$ .(b) Fermion condensate  $\langle \bar{\chi} \chi \rangle$ .Figure 6: Observables as functions of  $\beta$ .

lated conditions. Without loss of generality we restrict ourselves to the case of  $x = (1, 1, 1)^T$ . For improved statistics we consider a  $6^3$  lattice, where we sample the field configuration  $5 \times 10^4$  times. As an example we quote here

$$\text{Re} \langle L_0(x) \mathcal{O}_0(x, k) \rangle = 0.2258 \pm 0.0192, \quad (57)$$

$$\text{Re} \langle L_1(x) \mathcal{O}_1(x, k) \rangle = -0.0244 \pm 0.0049 \quad (58)$$

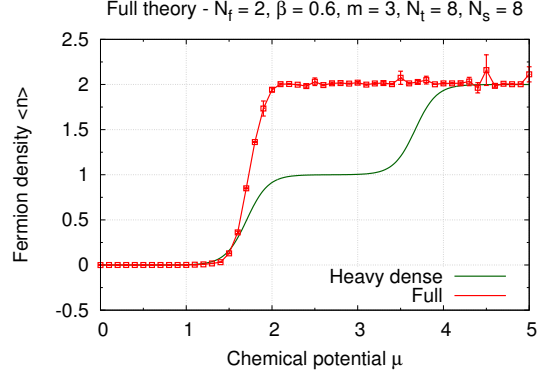
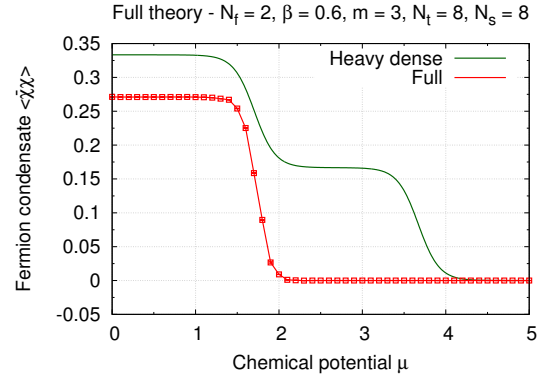
for  $\mathcal{I} = 0$ ,  $\mathcal{N} = \beta = m = \mu = k = 1$  for a violated condition. On the other hand,

$$\text{Re} \langle L_0(x) \mathcal{O}_0(x, k) \rangle = 0.0080 \pm 0.0058, \quad (59)$$

$$\text{Re} \langle L_1(x) \mathcal{O}_1(x, k) \rangle = -0.0004 \pm 0.0059 \quad (60)$$

for  $\mathcal{I} = 0$ ,  $\mathcal{N} = m = \mu = k = 1$ ,  $\beta = 10$  is an example for a condition which is compatible with a vanishing value. As usual,  $\mathcal{N}$  denotes the number of staggered fermion flavors,  $\mathcal{I}$  the imaginary noise,  $\beta$  the inverse coupling constant,  $m$  the mass and  $\mu$  the chemical potential.

If we take the error bounds estimated from the bootstrap analysis seriously, we observe several violations of

(a) Fermion density  $\langle n \rangle$ .(b) Fermion condensate  $\langle \bar{\chi} \chi \rangle$ .Figure 7: Observables for  $\mathcal{N} = 2$  degenerated flavors.

the consistency conditions in  $2 + 1$  dimensions. This is in agreement with the  $(0 + 1)$ -dimensional case, where many consistency conditions seem to be unfulfilled. We take this as a hint that the complex Langevin evolution in this canonical implementation might not converge correctly.

## G. Imaginary noise

We discussed in Sec. IIC how we can generalize from a real to an imaginary noise term, assuming correct convergence of the complex Langevin evolution. In this case observables should turn out to be independent of the noise term  $\mathcal{I}$ . However, in Fig. 8 we can find clear evidence for a dependence. Furthermore, we observe for almost all  $\mathcal{I} > 0$  a significantly larger deviation from analytical results. Hence, it was also not possible to fine-tune  $\mathcal{I}$  to a value so that the complex Langevin evolution yields correct results.

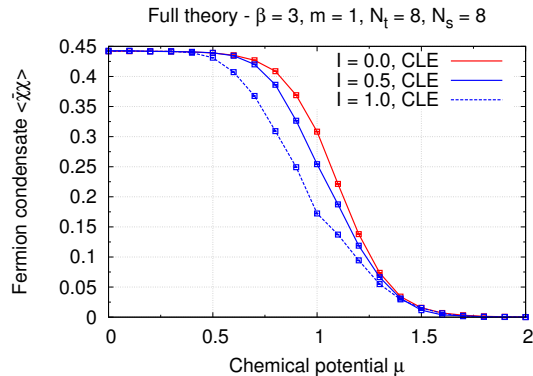


Figure 8: Condensate  $\langle \bar{\chi}\chi \rangle$  with imaginary noise  $\mathcal{I}$ .

### H. Analyticity in $\mu^2$

In Fig. 9 we find the condensate  $\langle \bar{\chi}\chi \rangle$  as a function of  $\mu^2$ . While for  $\mu^2 > 0$  the numerical evaluation employs a complex Langevin evolution, for  $\mu^2 \leq 0$  we use a real one. For small  $\beta$  the numerical evaluation tends to be unstable. Like in the  $(0+1)$ -dimensional case  $\langle \bar{\chi}\chi \rangle$  is analytic within the numerical accuracy. This suggests that the method can work sufficiently well for small  $\mu$ .

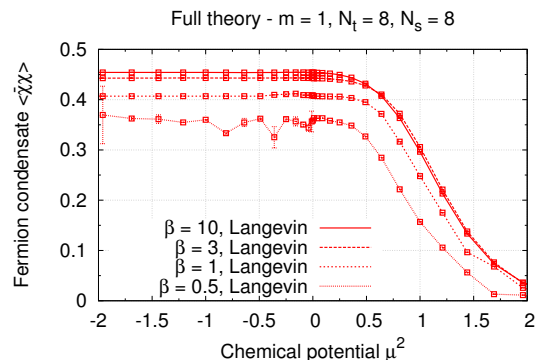
## V. CONCLUSIONS

In this paper we have extended our  $(0+1)$ -dimensional investigation of the generalized Thirring model in [29] to the  $(2+1)$ -dimensional case. The numerical findings are similar to those obtained in  $0+1$  dimensions. The complex Langevin evolution allows us to evaluate observables in the full theory in a straightforward way, despite the severe sign problem. However, our investigation suggests that in some cases it does not converge towards the physical theory. This was indicated by several violated consistency conditions, a gap in analytical predictions in the heavy dense limit and the absence of plateaus in the observables for  $\mathcal{N} > 1$  flavors.

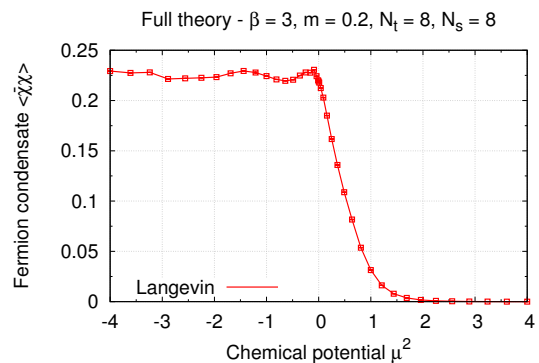
Despite these observations, we found the condensate  $\langle \bar{\chi}\chi \rangle$  to be analytical at  $\mu^2 = 0$ , suggesting that a complex Langevin evolution seems to work for small  $\mu$ . Also, for large  $\beta$  the heavy dense limit results could be reproduced. In these regimes we then have an appealing method to tackle the sign problem in the generalized Thirring model.

Further investigations have to deal with the question

of how to address the aforementioned problems. In particular, coordinate transformations as suggested in [58] and gauge-cooling procedures like the one employed in [59] might allow a stabilization of the complex Langevin evolution.



(a) Mass  $m = 1$  at varying  $\beta$ .



(b) Mass  $m = 0.2$  at  $\beta = 3$ .

Figure 9: Condensate  $\langle \bar{\chi}\chi \rangle$  as a function of  $\mu^2$ .

## ACKNOWLEDGMENTS

We thank I.-O. Stamatescu for many helpful remarks and clarifying discussions. We thank G. Aarts, D. Sexty and E. Seiler for discussions. This work is supported by the Helmholtz Alliance Grant No. HA216/EMMI and by Grand No. ERC-AdG-290623. C. Z. thanks the German National Academic Foundation for financial support.

[1] P. de Forcrand, PoS **LAT2009**, 010 (2009), [arXiv:1005.0539 \[hep-lat\]](https://arxiv.org/abs/1005.0539).

[2] M. P. Lombardo, *Mod.Phys.Lett.* **A22**, 457 (2007), [arXiv:hep-lat/0509180 \[hep-lat\]](https://arxiv.org/abs/hep-lat/0509180).

- [3] G. Aarts, PoS **LATTICE2012**, 017 (2012), [arXiv:1302.3028 \[hep-lat\]](#).
- [4] G. Aarts, PoS **LAT2009**, 024 (2009), [arXiv:0910.3772 \[hep-lat\]](#).
- [5] Y. D. Mercado, C. Gattringer, and A. Schmidt, *Comput.Phys.Commun.* **184**, 1535 (2013), [arXiv:1211.3436 \[hep-lat\]](#).
- [6] A. Schmidt, Y. D. Mercado, and C. Gattringer, PoS **LATTICE2012**, 098 (2012), [arXiv:1211.1573 \[hep-lat\]](#).
- [7] A. Alexandru and U. Wenger, *Phys.Rev.* **D83**, 034502 (2011), [arXiv:1009.2197 \[hep-lat\]](#).
- [8] A. Alexandru, M. Faber, I. Horvath, and K.-F. Liu, *Phys.Rev.* **D72**, 114513 (2005), [arXiv:hep-lat/0507020 \[hep-lat\]](#).
- [9] G. Parisi and Y. Wu, *Sci.Sin.* **24**, 483 (1981).
- [10] G. Parisi, *Phys.Lett.* **B131**, 393 (1983).
- [11] P. H. Damgaard and H. Huffel, *Phys.Rept.* **152**, 227 (1987).
- [12] F. Karsch and H. W. Wyld, *Phys.Rev.Lett.* **55**, 2242 (1985).
- [13] G. Aarts and F. A. James, *JHEP* **1201**, 118 (2012), [arXiv:1112.4655 \[hep-lat\]](#).
- [14] N. Bilic, H. Gausterer, and S. Sanielevici, *Phys.Rev.* **D37**, 3684 (1988).
- [15] G. Aarts and I.-O. Stamatescu, *JHEP* **0809**, 018 (2008), [arXiv:0807.1597 \[hep-lat\]](#).
- [16] G. Aarts and K. Splittorff, *JHEP* **1008**, 017 (2010), [arXiv:1006.0332 \[hep-lat\]](#).
- [17] G. Aarts, *Phys.Rev.Lett.* **102**, 131601 (2009), [arXiv:0810.2089 \[hep-lat\]](#).
- [18] G. Aarts, *JHEP* **0905**, 052 (2009), [arXiv:0902.4686 \[hep-lat\]](#).
- [19] J. Berges and I.-O. Stamatescu, *Phys.Rev.Lett.* **95**, 202003 (2005), [arXiv:hep-lat/0508030 \[hep-lat\]](#).
- [20] J. Berges, S. Borsanyi, D. Sexty, and I.-O. Stamatescu, *Phys.Rev.* **D75**, 045007 (2007), [arXiv:hep-lat/0609058 \[hep-lat\]](#).
- [21] J. Berges and D. Sexty, *Nucl.Phys.* **B799**, 306 (2008), [arXiv:0708.0779 \[hep-lat\]](#).
- [22] J. Ambjorn, M. Flensburg, and C. Peterson, *Nucl.Phys.* **B275**, 375 (1986).
- [23] G. Aarts and F. A. James, *JHEP* **1008**, 020 (2010), [arXiv:1005.3468 \[hep-lat\]](#).
- [24] H. W. Hamber and H. Ren, *Phys.Lett.* **B159**, 330 (1985).
- [25] J. Flower, S. W. Otto, and S. Callahan, *Phys.Rev.* **D34**, 598 (1986).
- [26] E.-M. Ilgenfritz, *Phys.Lett.* **B181**, 327 (1986).
- [27] D. Spielmann, *Aspects of confinement in QCD from lattice simulations*, Ph.D. thesis, Ruprecht-Karls-Universität Heidelberg (2010).
- [28] H. Gies and L. Janssen, *Phys.Rev.* **D82**, 085018 (2010), [arXiv:1006.3747 \[hep-th\]](#).
- [29] J. M. Pawłowski and C. Zielinski, *Phys.Rev.* **D87**, 094503 (2013), [arXiv:1302.1622 \[hep-lat\]](#).
- [30] I. Bender, T. Hashimoto, F. Karsch, V. Linke, A. Nakamura, *et al.*, *Nucl.Phys.Proc.Suppl.* **26**, 323 (1992).
- [31] G. Aarts, E. Seiler, and I.-O. Stamatescu, *Phys.Rev.* **D81**, 054508 (2010), [arXiv:0912.3360 \[hep-lat\]](#).
- [32] G. Aarts, F. A. James, E. Seiler, and I.-O. Stamatescu, *Eur.Phys.J.* **C71**, 1756 (2011), [arXiv:1101.3270 \[hep-lat\]](#).
- [33] G. Aarts, F. A. James, E. Seiler, and I.-O. Stamatescu, PoS **LATTICE2011**, 197 (2011), [arXiv:1110.5749 \[hep-lat\]](#).
- [34] W. E. Thirring, *Annals Phys.* **3**, 91 (1958).
- [35] S. Christofi, S. Hands, and C. Strouthos, *Phys.Rev.* **D75**, 101701 (2007), [arXiv:hep-lat/0701016 \[hep-lat\]](#).
- [36] T. D. Cohen, *Phys.Rev.Lett.* **91**, 222001 (2003), [arXiv:hep-ph/0307089 \[hep-ph\]](#).
- [37] J. B. Kogut and L. Susskind, *Phys.Rev.* **D11**, 395 (1975).
- [38] T. Banks, L. Susskind, and J. B. Kogut, *Phys.Rev.* **D13**, 1043 (1976).
- [39] T. Banks *et al.* (Cornell-Oxford-Tel Aviv-Yeshiva Collaboration), *Phys.Rev.* **D15**, 1111 (1977).
- [40] L. Susskind, *Phys.Rev.* **D16**, 3031 (1977).
- [41] P. Hasenfratz and F. Karsch, *Phys.Lett.* **B125**, 308 (1983).
- [42] S. R. Sharpe, PoS **LAT2006**, 022 (2006), [arXiv:hep-lat/0610094 \[hep-lat\]](#).
- [43] L. Del Debbio and S. Hands, *Phys.Lett.* **B373**, 171 (1996), [arXiv:hep-lat/9512013 \[hep-lat\]](#).
- [44] J. Han and M. A. Stephanov, *Phys.Rev.* **D78**, 054507 (2008), [arXiv:0805.1939 \[hep-lat\]](#).
- [45] J. O. Andersen, L. T. Kyllingstad, and K. Splittorff, *JHEP* **1001**, 055 (2010), [arXiv:0909.2771 \[hep-lat\]](#).
- [46] J. Ambjorn and S. K. Yang, *Phys.Lett.* **B165**, 140 (1985).
- [47] G. Aarts, F. A. James, E. Seiler, and I.-O. Stamatescu, *Phys.Lett.* **B687**, 154 (2010), [arXiv:0912.0617 \[hep-lat\]](#).
- [48] T. C. Blum, J. E. Hetrick, and D. Toussaint, *Phys.Rev.Lett.* **76**, 1019 (1996), [arXiv:hep-lat/9509002 \[hep-lat\]](#).
- [49] J. Engels, O. Kaczmarek, F. Karsch, and E. Laermann, *Nucl.Phys.* **B558**, 307 (1999), [arXiv:hep-lat/9903030 \[hep-lat\]](#).
- [50] G. Aarts, O. Kaczmarek, F. Karsch, and I.-O. Stamatescu, *Nucl.Phys.Proc.Suppl.* **106**, 456 (2002), [arXiv:hep-lat/0110145 \[hep-lat\]](#).
- [51] K. Fukushima and Y. Hidaka, *Phys.Rev.* **D75**, 036002 (2007), [arXiv:hep-ph/0610323 \[hep-ph\]](#).
- [52] R. Hofmann and I.-O. Stamatescu, *Nucl.Phys.Proc.Suppl.* **129**, 623 (2004), [arXiv:hep-lat/0309179 \[hep-lat\]](#).
- [53] R. De Pietri, A. Feo, E. Seiler, and I.-O. Stamatescu, *Phys.Rev.* **D76**, 114501 (2007), [arXiv:0705.3420 \[hep-lat\]](#).
- [54] D. Banerjee and S. Chandrasekharan, *Phys.Rev.* **D81**, 125007 (2010), [arXiv:1001.3648 \[hep-lat\]](#).
- [55] M. Abramowitz and I. Stegun, *Handbook of Mathematical Functions with Formulas, Graphs, and Mathematical Tables*, Applied mathematics series No. Bd. 55, Nr. 1972 (U.S. Govt. Print. Off., 1964).
- [56] M. Galassi, J. Davies, J. Theiler, B. Gough, G. Jungman, P. Alken, M. Booth, and F. Rossi, *GNU Scientific Library Reference Manual* (Network Theory, 2009).
- [57] T. DeGrand and C. E. Detar, *Lattice methods for quantum chromodynamics* (World Scientific, 2006).
- [58] G. Aarts, F. A. James, J. M. Pawłowski, E. Seiler, D. Sexty, *et al.*, *JHEP* **1303**, 073 (2013), [arXiv:1212.5231 \[hep-lat\]](#).
- [59] E. Seiler, D. Sexty, and I.-O. Stamatescu, (2012), [arXiv:1211.3709 \[hep-lat\]](#).